Superstable ultra-thin water film confined in a hydrophilized carbon nanotube

Yoko Tomo,[1,2] Alexandros Askounis,[2,3] Tatsuya Ikuta,[1,2] Yasuyuki Takata,[2,3] Khellil Sefiane[4] and Koji Takahashi[1,2]*

[1]Department of Aeronautics and Astronautics, Graduate School of Engineering, Kyushu University, 744 Motooka, Nishi-ku, Fukuoka 819-0395, Japan

[2]International Institute for Carbon-Neutral Energy Research (WPI-I2CNER), Kyushu University, 744 Motooka, Nishi-ku, Fukuoka 819-0395, Japan

[3]Department of Mechanical Engineering, Graduate School of Engineering, Kyushu University, 744 Motooka, Nishi-ku, Fukuoka 819-0395, Japan

[4]Institute for Multiscale Thermofluids, School of Engineering, The University of Edinburgh, King's Buildings, Robert Stevenson Road, Edinburgh EH9 3FB, UK

ABSTRACT

Fluids confined in a nanoscale space behave differently than in the bulk due to strong interactions between fluid molecules and solid atoms. Here, we observed water confined inside "open" hydrophilized carbon nanotubes (CNT), with diameter of tens of nanometers, using transmission electron microscopy (TEM). A 1-7 nm water films adhering to most of the inner wall surface was

observed and remained stable in the high vacuum (order of 10^{-5} Pa) of the TEM. The super-stability of this film was attributed to a combination of curvature, nano-roughness and confinement resulting in a lower vapor pressure for water and hence inhibiting its vaporization. Occasional, suspended ultra-thin water film with thickness of 3-20 nm were found and remained stable inside the CNT. This film thickness is one order of magnitude smaller than the critical film thickness (about 40 nm) reported by the DLVO theory and previous experimental investigations. The stability of the suspended ultra-thin water film is attributed to the additional molecular interactions due to the extended water meniscus, which balances the rest of the disjoining pressures.

KEYWORDS

Carbon nanotube, water, transmission electron microscopy, thin liquid film, and disjoining pressure

Carbon nanotubes (CNTs) were first reported by Iijima in 1991.[1] Since then, their unique properties have been unveiled and extensively studied, for example, high mechanical strength[2] and exceptional thermal[3–5] and electrical conductivity.[6,7] In addition, the hollow core of the CNTs can be utilized in applications such as drug delivery, desalination and nano-filtration.[8–11] Nonetheless, the dynamics of fluids within nanoscale confinement is far from understood and has received considerable attention recently leading to the emerging field of nanofluidics. The major question in nanofluidics is the extent to which classical equations describing fluid behavior remain valid under nanoscale confinement. Under nanoscale confinement, such as inside the core of CNTs, the interactions between the liquid and solid atoms become dominant. Molecular dynamics (MD) have

played a vital role in understanding these interactions. In particular, the extremely fast transport of wetting fluids through CNTs is predicted by MD simulations[12,13] and confirmed by experimental measurements.[14–16] Essentially, the confinement of the liquid and the smooth wall results in large slip on the wall which in turn enhances the flow velocity inside CNTs. The situation is more complex for water due to hydrogen bonding. The structure of water changes due to strong hydrogen-bonded networks, which cause an increase of freezing point of water inside CNTs with diameters of 1-2 nanometers.[17,18] Although MD simulations is an established powerful approach to investigate the influence of liquid-wall interactions on the dynamic behavior of liquids, experimental validation is still required.

To resolve these phenomena and outstanding issues within CNTs area, electron microscopy should be used. In fact, environmental scanning electron microscopy (ESEM) allowed in-situ observation of water phase change within open-capped CNTs, providing some necessary experimental evidence.[19,20] However, the spatial resolution of ESEM is inadequate to visualize the liquid structure in the nano-confinement. Transmission electron microscopy (TEM) has higher, sub-nanometer spatial resolution. Nonetheless, TEM operates in high vacuum (~10^{-5} Pa) leading to quick evaporation of most fluids. Therefore, previous studies of nano-confined water have been limited to the use of liquid cells[21–23] or closed-capped CNTs, which maintain their inner pressure at atmospheric level.[24,25]

In this contribution, we employed TEM to investigate the effect of liquid-wall interactions on the formation of ultra-thin water films on the wall of "open" CNTs. These ultra-thin films are 1-7 nm thick. Unexpectedly, these films remain stable and do not evaporate under the vacuum condition of the TEM, due to a combination of strong liquid adhesion to the wall and the great effect of the nanoscale confinement. Moreover, for the first time, we found suspended ultra-thin

liquid films which are stable inside the CNTs. Their thickness is 3-20 nm, which is an order of magnitude smaller than previously reported.[26] To discuss the physical mechanisms of water stability in vacuum, we combined the Kelvin equation with a disjoining pressure formula, incorporating the nanoscale roughness characteristics of the wall. Moreover we discuss the stability of suspended ultra-thin water films using DLVO (Derjaguin-Landau-Verwey-Overbeek) theory. Our observations indicate that hydrophilized CNTs have great potential for novel applications for *in-situ* TEM observations, for example, chemical and biological reactions, and phase-change of water confined within nano-spaces.

Figure 1 (a) and (b) exhibit the first, to the best of our knowledge, experimental observation of stable ultra-thin films in open-sided, hollow carbon nanomaterials. Detailed characterization of the nanomaterial is provided in Methods. In the supporting information, Figure S1 and S2 depict separate electron beam prolonged-irradiation experiments and elemental analysis by electron energy loss spectroscopy (EELS), respectively, demonstrating that the observed films are indeed liquid films of pure water. The ultra-thin films were found mainly on the walls and occasionally suspended from the walls. The former lies on the surface of the CNT wall, with one surface of the ultra-thin film facing the vacuum and the other adhering to the solid (CNT wall), as shown in Figure 1 (a). The latter ultra-thin film is supported by the CNT wall and both sides of the surface of the film face vacuum. Previous observations, were limited to either closed-capped CNTs[24,25] or infused with molten metals which maintains the environment ambient conditions.[27] This result demonstrates an enhanced stability of water films in CNTs even though water is exposed to vacuum (10^{-5} Pa). In what follows, we attempt to discuss in detail the stability mechanism for these ultra-thin water films.

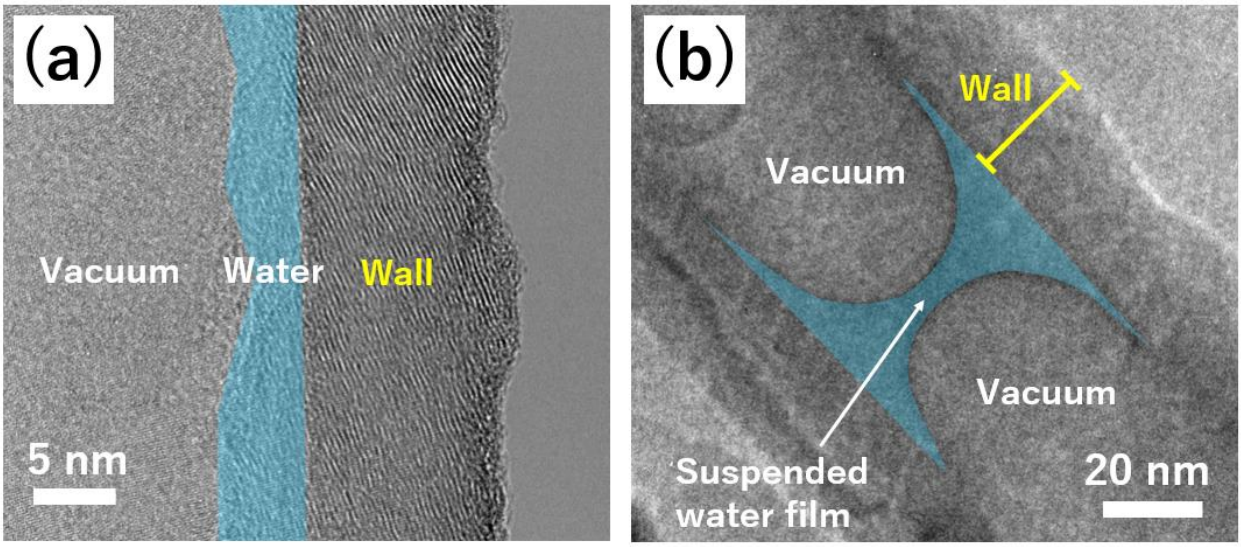

Figure 1. TEM micrographs of (a) An ultra-thin water film lying on the surface of the CNT. (b) A suspended ultra-thin water film. Thin water films are colored blue for better contrast.

Let us first consider the ultra-thin film adhering to the CNT wall, depicted in Figure 1(a). The curvature of a solid-liquid interface should reduce the vapor pressure of the liquid and slow its evaporation when confined and the liquid-vacuum interface attains a concave shape. The liquid vapor pressure as a function of curvature can be described by Kelvin equation as:[28]

$$\ln\frac{P_{ve}}{P_{sat}} = \left(\frac{1}{r_1}+\frac{1}{r_2}\right)\frac{\sigma V_m}{RT} \qquad (1)$$

where, P_{ve} is the equilibrium vapor pressure on a curved liquid-gas interface, P_{sat} is the saturated vapor pressure on a flat liquid-gas interface, σ is the surface tension, V_m is the molar volume of liquid, R is the gas constant, T is the temperature. r_1 and r_2 are the radius of perpendicular curvatures of the liquid-gas interface. Previously, Kelvin equation accurately

explained the stability of a microscale droplet due to super saturation on its convex liquid-gas interface.[28] In the case of a bubble, the concave shape of the liquid-gas interface results in the parameters within the parenthesis in the right hand side, which is the curvature, being negative.[29]

For the film adhering to the inner CNT wall, we assume temperature to remain constant at 300 K, as temperature rise is minimal during TEM observation at this magnification.[30] For $T = 300$ K, $P_{sat} = 3.6\times10^{3}$ Pa, $\sigma = 72$ mN/m, $V_m = 1.8\times10^{-5}$ m^3/mol and $R = 8.31$ J/K/mol. $r_1 = \infty$, as there is no curvature in the axial direction and the curvature in the radial direction, r_2, is the CNT radius minus the film thickness, which is extracted from Figure 1 (a) to be $r_2 = 21$ nm. In our case, the curvature of liquid-vacuum interface is concave, making the right side of equation (1) negative.[29] For 300 K, $P_{ve} = 3.5\times10^{3}$ Pa, which is lower than P_{sat} and hence water does not evaporate at atmospheric pressure, but this P_{ve} does not explain why water remains stable within the CNT even at the vacuum of the TEM (10^{-5} Pa).

Although equation 1 describes sufficiently the liquid vapor pressure, P_{ve}, at room conditions, it cannot account for lower pressure environments and vacuum in particular. We believe that nano-confinement within the CNTs renders both liquid-wall interactions and wall roughness key parameters for the stability of the ultra-thin water films we observed.

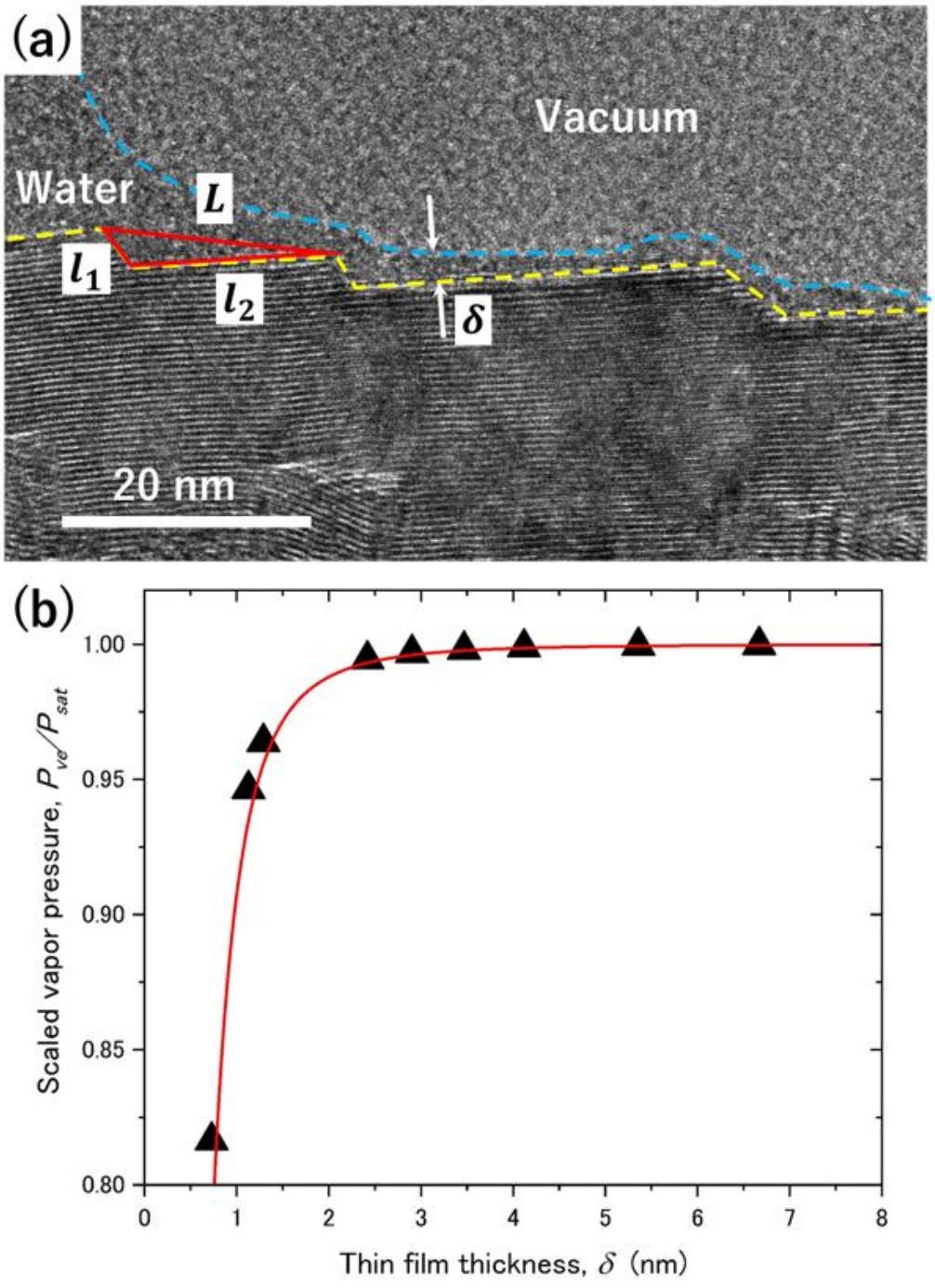

Figure 2. (a) TEM micrograph of the triangular structures filled with water molecules. The yellow dot line indicates the wall-water interface. The blue dot line indicates the water-vacuum interface. (b) Scaled vapor pressure due to disjoining pressure. Triangle plots are calculated from

experimental results by using r_w. The red solid line is calculated from our experimental results using the Hu *et al.* equation for comparison.[31]

Let us now consider the liquid-wall interactions which become increasingly important due to the nanoscale confinement. Figure 2 (a) exhibits a magnification of the liquid-wall contact area, where the cupped wall structure leads to a nanoscale roughness of the inner wall of the CNT. The liquid can be seen to fully wet these features, in a similar fashion to Wenzel wetting, resulting in strong water adhesion to the wall. At the same time, the strong liquid adhesion should further inhibit evaporation leading to low vapor pressure at the nanoscale confinement. We calculate the disjoining pressure Π, neglecting capillary pressure due to symmetry and incorporating the nano-roughness effect as follows:[31]

$$\Pi = -\rho k_B T \ln \frac{P_{ve}}{P_{sat}} \qquad (2)$$

The disjoining pressure $\Pi = A/6\pi\delta^{*3}$ is the excess pressure required to evaporate liquid molecules due to van der Waals forces. The Hamaker constant is $A_{\mathrm{Graphite-H_2O}} = 9.08\times10^{-20}$ J.[32] δ^* is the modified film thickness on the nano-rough surface calculated as $\delta^* = \delta/r_w$, where r_w is the Wenzel roughness ratio between the actual and flat surface areas. We measured the three lengths l_1, l_2, L of each triangular structure from the TEM images, as shown in Figure 2 (a), and then calculated $r_w = (l_1 + l_2)/L$. The scaled vapor pressure is plotted in Figure 2 (b) as a function of δ (triangles). These results are in agreement with previous model by Hu *et al*. of the influence of nanoscale roughness on the stability, P_{ve}, of the liquid film, indicated with the red line in Figure

2 (b).[31] In fact, we believe our results to be the first experimental observation corroborating these particular predictions. Although our calculations indicate that nanoscale roughness decreases the P_{ve} of the ultra-thin liquid films, the influence of the nanoscale roughness is not strong enough to explain the stability of the water in vacuum.

The last mechanism to maintain the water in vacuum is the enhanced interaction between water molecules and hydrophilized parts inside the CNT. Oxygen plasma treatment should render the wall surfaces denoted by l_1 in Figure 2 (a) hydrophilic locally. In particular, the pentagonal carbon rings at the edges of graphene layers should open rapidly with the plasma, and bond with oxygen groups, before the honeycomb structure (sp2) of the rest of the layer opens.[33] Therefore, the inner wall surface becomes more hydrophilic than the original CNTs, leading to stronger water-carbon interactions (lower P_{ve}), hindering liquid vaporization in the TEM vacuum. This finding has been predicted previously, using MD simulations. In particular, Chaban *et al.*, demonstrated that increasing water-carbon interactions lowers P_{ve}, which combined with the effect of confinement greatly inhibit evaporation.[34]

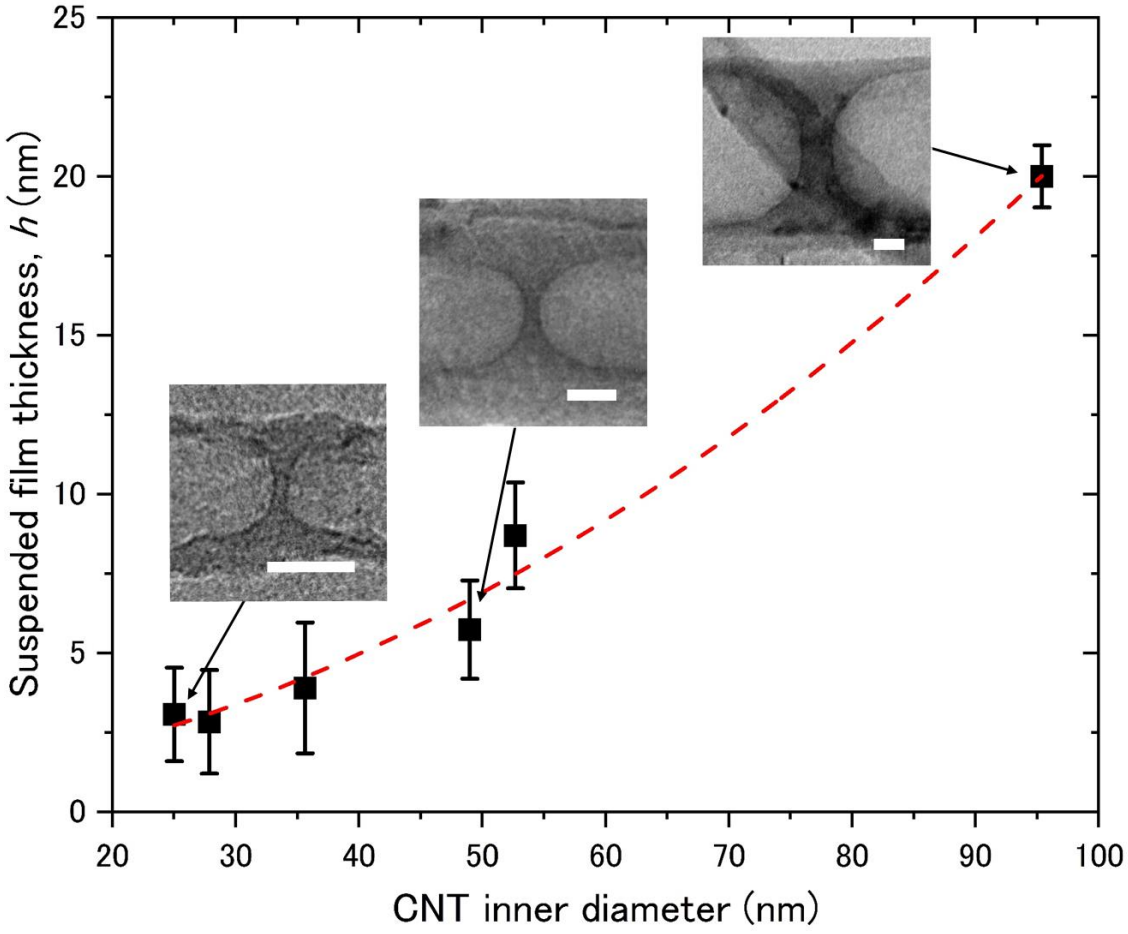

Figure 3. Suspended ultra-thin film thickness as a function of CNT inner diameter. The thickness plotted here is the minimum one on each CNT inner diameters. Scale bars indicate 20 nm.

Further to the unexpected ultra-thin water films adhered to the CNT walls, we observed occasional suspended ultra-thin water films, with thickness 3-20 nm inside the CNTs, shown in Figure 3 as a function of CNT inner diameter. Previous experiments and the DLVO theory indicate that a suspended water film will rupture if its thickness falls below 40 nm.[26] Notably, the water film thickness we observed here is one order of magnitude smaller than that at the microscale. We estimated the electrostatic and intermolecular interactions on the suspended ultra-thin water film using DLVO theory. The attractive and repulsive interactions between the two liquid-vacuum interfaces of the ultra-thin film acts against film thinning and hence render the film stable. The attractive interaction includes the van der Waals interaction, Π_{vdW}, and hydrophobic interactions, Π_{hb}. The repulsive interaction includes the electrostatic interactions, Π_{el}. Previously, Π_{hb} was attributed to strong interaction of water with air molecules. In our case, the film is suspended in vacuum, therefore Π_{hb} can be neglected. DLVO theory described Π_{vdW} quantitatively these interactions as:[28]

$$\Pi_{\mathrm{vdW}} = -\frac{A}{6\pi h^3} \qquad (3)$$

where A is the Hamaker constant of water film in vacuum $A_{\mathrm{H_2O}} = 3.7 \times 10^{-20}$ J from Lifshitz's theory[35] and h is the film thickness of the suspended water film.

$$\Pi_{\mathrm{el}} = 64 k_B T \rho_\infty \gamma^2 \mathrm{e}^{-\kappa h} \qquad (4)$$

with

$$\gamma = \tanh\left(\frac{e\psi_0}{4k_B T}\right) \qquad (5)$$

and

$$\kappa = \sqrt{\frac{2\rho_\infty e^2}{\varepsilon_0 \varepsilon k_B T}} \qquad (6)$$

, where e =1.602×10^{-19} C is the electron charge, ψ_0 is the surface potential of the film, k_B =1.381 ×10^{-23} J/K is the Boltzmann constant, and T is the temperature. κ is the inverse of the Debye length. ρ_∞ is the number density of ions, ε_0 = 8.854×10^{-12} F/m is the electric permittivity of vacuum, and ε is the relative dielectric constant of water. It is noted that even in deionized water, ions (H_3O^+ and OH^-) cannot be ignored.[28] For T = 300 K and the deionized water (The total ionic strength of water is $I = 2.5 \times 10^{-6}$ M),[26] $\psi_0 = -60 \pm 5$ mV, $\rho_\infty = 6.022 \times 10^{26} \times I$ /m^3, and ε is 77. Total disjoining pressure of the suspended water film, Π_{susp}, is given by:

$$\Pi_{\text{susp}} = \Pi_{\text{vdW}} + \Pi_{\text{el}} \qquad (7)$$

Each quantity is plotted as a function of h in Figure 4 (a). Additionally, we consider the driving capillary pressure, ΔP, as:[26]

$$\Delta P = P_C - \Pi_{\text{susp}} \qquad (8)$$

, where capillary pressure is $P_C = 2\sigma/r_m$, σ is the surface tension of the liquid-gas interface and r_m is the radius of curvature of the meniscus. Essentially, ΔP is the balance between P_C and Π_{susp} at the two plane-parallel surfaces of the film and stable films should be attained when ΔP = 0. However, our calculations show that $\Delta P > 0$, for r_m= 25 nm, P_C = 5.8×10^6 Pa. In the range of 3 nm < h < 20 nm, Π_{susp} is considerably smaller than P_C, corresponding to the gray area in Figure 4 (a). A similar result has been predicted by Lech *et al.*[26] using the same theoretical approach,

albeit for thicker films. In particular, they were capable of accurately describing the thickness of films with small or large charges, nonetheless pure deionized water deviated greatly, possibly due to divergence in Π_{el}. In the supporting information we attempt to theoretically predict the influence of Π_{el} on the meniscus shape. Nonetheless, the exact role of Π_{el} merits to be revisited both experimentally and theoretically in the future.

Moreover, we should consider the effect of confinement on the intermolecular interactions. The DLVO theory[26] assumes two infinite plane-parallel surfaces, where interactions exist only between water molecules (blue spheres) in the plane-surface, as indicated with white arrows in Figure 4 (b). Inside the CNT, the length of the plane-parallel surfaces is very limited as indicated by the dashed lines and is surrounded by the meniscus which brings additional water molecules closer together. In turn, these additional water molecules interact with the ones within the dashed lines, enhancing the overall water-water interactions as highlighted by the red arrows in Figure 4 (c). Therefore, the extra forces from the meniscus molecules will counter the strong Π_{vdW} moving Π_{susp} to a stable position. Interestingly, Π_{susp} in CNTs should be much higher than Π_{susp} from the DLVO theory.

Let us now focus on the apparent *h* dependence on the inner diameter of the CNT, due to the force balance in a suspended water film, as shown in Figure 3. Arising from the above analysis, the attractive force is due to the capillary pressure and the repulsive one is due to Π_{susp}. Therefore, the two water-vacuum interfaces of the suspended water film will move until the attractive force balances the repulsive one. The capillary pressure and disjoining pressure are a function of the radius of the curvature of the meniscus and the suspended film thickness respectively, indicating that the stable film thickness depends on the inner diameter of CNT.

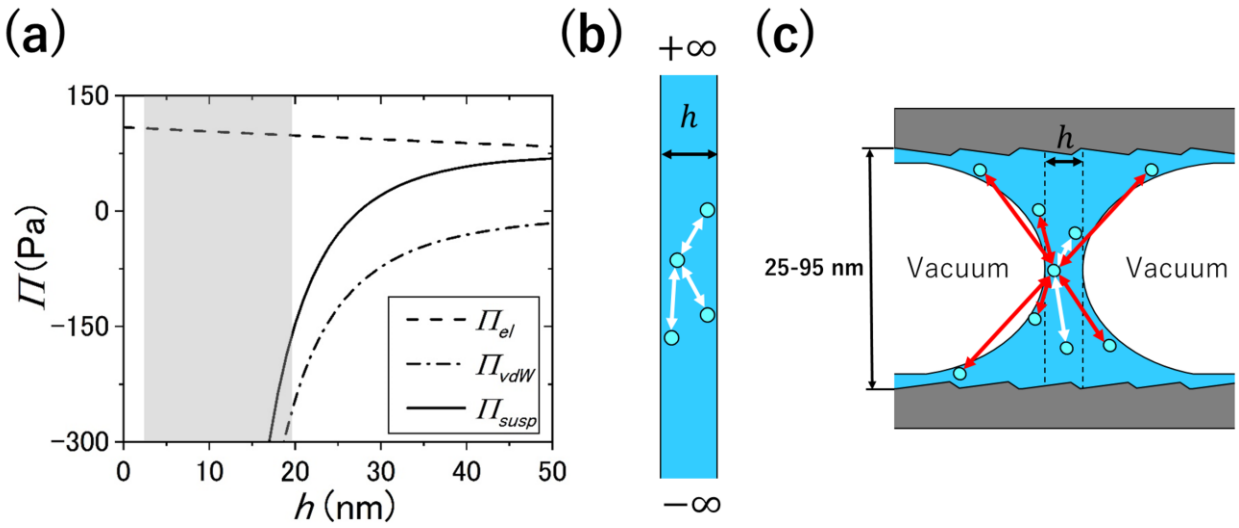

Figure 4. (a) Plot of Π_{susp} and its components as a function of h. The grey area defines the range of the suspended film thickness observed in our experiments. (b) Schematic illustrations of infinite plane-parallel surfaces assumed in the DLVO theory.[26] (c) A suspended ultra-thin water film in a CNT. In both (b) and (c), blue circles are water molecules and white arrows indicate water-water interactions in the plane-parallel configuration. Red arrows indicate molecular interactions between water molecules in the plane-parallel configuration with those in the meniscus.

In summary, we report for the first time the experimental observation of super-stable ultra-thin water film within "open-sided" CNTs using TEM. Two distinct types of films were observed. One adhering to the CNT wall due to a combination of the effect of confinement, curvature and hydrophilicity on the disjoining pressure. These parameters lower the vapor pressure and inhibit vaporization even in vacuum. The second film was found to be occasionally suspended between the walls. The stability of this type of ultra-thin water film was attributed to a balance between capillary pressure and disjoining pressure, which was achieved by the formation of the meniscus. The meniscus brings more water molecules closer together which interact and essentially balance the forces acting on the film. These films are one order of magnitude smaller than previous

experimental observations[26] and exist in vacuum. The unexpected stability and ultra-thin films of water inside the CNTs should pave the way for advancements in the understanding of nanofluidics of water. These results should advance our understanding of water behavior in confinement at the nanoscale and open the door for new applications such as drug delivery and nanoscale phase-change heat transfer.

Methods

Carbon nanotubes in powder form were hydrophilized to increase their solubility in water with oxygen plasma treatment (Yamato Kagaku, Japan, 60W, 70ml/min, 20 min), added to deionized water and sonicated until suspended. Subsequently, a drop of the suspension was deposited on a TEM grid (Structure Probe. Inc., West Chester, PA, USA) of a Si (100) substrate with a silicon nitride membrane window, and left to dry in a clean room overnight. The grid was also hydrophilized with oxygen plasma treatment, in order to increase the wettability by the suspension droplet and avoid CNT agglomeration on the grid. Visualization was conducted with a TEM (JEM-3200FSK, JEOL Ltd., Tokyo, Japan) operated at 300 kV. Cup-stacked type carbon nanotubes with high temperature treatment[36] were chosen for this study due to their open ends, as shown in Figure 5 (a). They exhibit a unique wall structure of graphene layers rolled-up into cones and stacked inside each other with a hollow core, as shown in Figure 5 (b), similar to previous reports.[37,38] Moreover, oxygen treatment renders the ends of the graphene layers hydrophilic,[33] although the protruding edges increase wall roughness (inset of Figure 5 (b)). Before and after every observation, we confirmed that both ends of CNT were open. We successfully inserted water inside the CNTs, as shown in Figure 1 (a) and (b) via capillary action. The surface tension of water is 72 mN/m, which is well below the wetting limit for carbon nanomaterials of 100-200 mN/m.[39] In our

samples, we used deionized water and samples were kept in hermitically closed boxes, in a clean room environment. They were not in the vicinity of salts, hence the observed liquid films should be of pure water. To verify, we captured the change of the suspended film thickness and the film rupture over prolonged periods of time due to electron beam irradiation, as depicted in Figure S1. Water purity was verified by EELS, as shown in Figure S2.

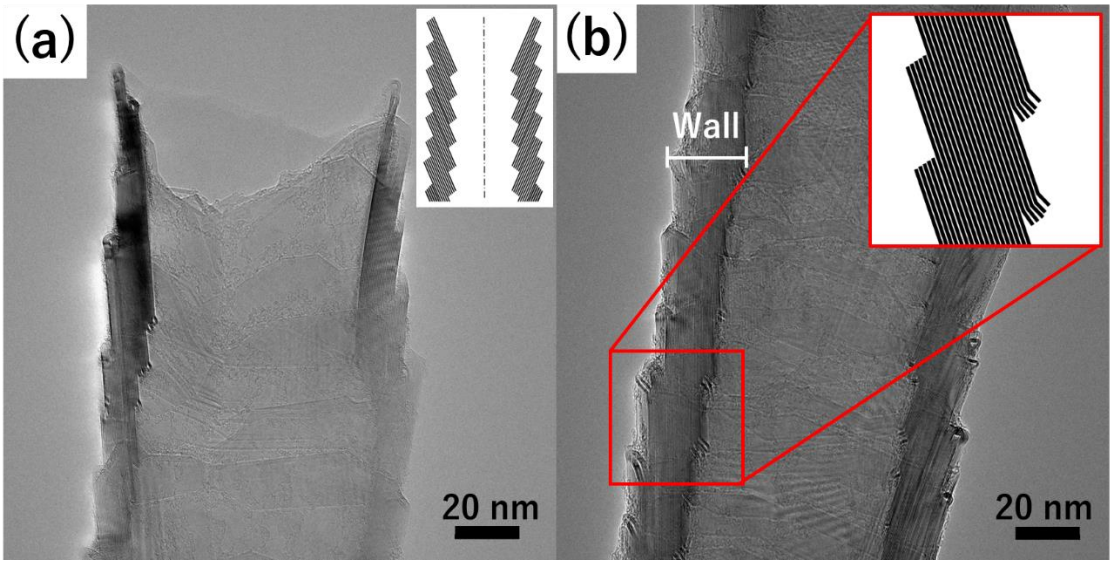

Figure 5. TEM micrographs demonstrating (a) the open end of an empty CNT and (b) a middle section of the same CNT. The inner wall of the CNT exhibits nanoscale roughness due to the edges of the cups. Insets schematically illustrate the cupped wall structure and the nano-roughness.

AUTHOR INFORMATION

Corresponding Author

*E-mail: takahashi@aero.kyushu-u.ac.jp

Supporting Information Available

Observation of electron beam irradiating the suspended thin film and leading to its rupture. Elemental analysis of empty and water-filled CNTs with EELS proving existence of water. Prediction of ionic strength influence on the suspended film shape and thickness.

ACKNOWLEDGMENTS

This work was partially supported by JSPS KAKENHI (JP16K14174, JP16H04280, JP16H02315, JP17H03186). TEM observations were performed at the Ultramicroscopy Research Center, Kyushu University.

REFERENCES

(1) Iijima, S. *Lett. to Nat.* **1991**, *353*, 737–740.

(2) Treacy, M. M. J.; Ebbesen, T. W.; Gibson, J. M. *Lett. to Nat.* **1996**, *381*, 678–680.

(3) Yu, C.; Shi, L.; Yao, Z.; Li, D.; Majumdar, A. *Nano Lett.* **2005**, *5*, 1842–1846.

(4) Kim, P.; Shi, L.; Majumdar, A.; McEuen, P. L. *Phys. Rev. Lett.* **2001**, *87*, 215502.

(5) Fujii, M.; Zhang, X.; Xie, H.; Ago, H.; Takahashi, K.; Ikuta, T.; Abe, H.; Shimizu, T. *Phys. Rev. Lett.* **2005**, *95*, 65502.

(6) Dekker, C. *Phys. Today* **1999**, *52*, 22–28.

(7) Wildöer, J. W. G.; Venema, L. C.; Rinzler, A. G.; Smalley, R. E.; Dekker, C. *Nature* **1998**, *391*, 59–62.

(8) Bianco, A.; Kostarelos, K.; Prato, M. *Curr. Opin. Chem. Biol.* **2005**, *9*, 674–679.

(9) Joshi, R. K.; Carbone, P.; Wang, F. C.; Kravets, V. G.; Su, Y.; Grigorieva, I. V.; Wu, H. A.; Geim, A. K.; Nair, R. R. *Science (80-.).* **2014**, *343*, 752–754.

(10) Kasu, M.; Makimoto, T.; Balakrishnan, K.; Katona, T.; Ploog, K. H.; Johnson, N. M.; Walker, J.; Bour, D. P.; Street, R. A.; Grudowski, P. A.; Dupuis, R. D.; Fiorentini, V.; Vanderbilt, D.; Jena, D. *Science (80-.).* **2010**, *327*, 64–68.

(11) Geng, J.; Kim, K.; Zhang, J.; Escalada, A.; Tunuguntla, R.; Comolli, L. R.; Allen, F. I.; Shnyrova, A. V.; Cho, K. R.; Munoz, D.; Wang, Y. M.; Grigoropoulos, C. P.; Ajo-Franklin, C. M.; Frolov, V. A.; Noy, A. *Nature* **2014**, *514*, 612–615.

(12) Hummer, G.; Rasaiah, J. C.; Noworyta, J. P. *Nature* **2001**, *414*, 188–190.

(13) Falk, K.; Sedlmeier, F.; Joly, L.; Netz, R. R.; Bocquet, L. *Nano Lett.* **2010**, *10*, 4067–4073.

(14) Holt, J. K.; Park, H. G.; Wang, Y.; Stadermann, M.; Artyukhin, A. B.; Grigoropoulos, C. P.; Noy, A.; Bakajin, O. *Science (80-.).* **2006**, *312*, 1034–1037.

(15) Whitby, M.; Quirke, N. *Nat. Nanotechnol.* **2007**, *2*, 87–94.

(16) Secchi, E.; Marbach, S.; Niguès, A.; Stein, D.; Siria, A.; Bocquet, L. *Nature* **2016**, *537*, 210–213.

(17) Koga, K.; Gao, G. T.; Tanaka, H.; Zeng, X. C. *Nature* **2001**, *412*, 802–805.

(18) Agrawal, K. V.; Shimizu, S.; Drahushuk, L. W.; Kilcoyne, D.; Strano, M. S. *Nat. Nanotechnol.* **2016**, *12*, 267–273.

(19) Mattia, D.; Gogotsi, Y. *Microfluid. Nanofluidics* **2008**, *5*, 289–305.

(20) Pía Rossi, M.; Ye, H.; Gogotsi, Y.; Babu, S.; Ndungu, P.; Bradley, J. C. *Nano Lett.* **2004**, *4*, 989–993.

(21) Shin, D.; Park, J. B.; Kim, Y.; Kim, S. J.; Kang, J. H.; Lee, B.; Cho, S.-P.; Hong, B. H.; Novoselov, K. S. *Nat. Commun.* **2015**, *6*, 6068.

(22) Ross, F. M. *Science (80-.).* **2015**, *350*, aaa9886.

(23) Tomo, Y.; Takahashi, K.; Nishiyama, T.; Ikuta, T.; Takata, Y. *Int. J. Heat Mass Transf.* **2017**, *108*, 1460–1465.

(24) Naguib, N.; Ye, H.; Gogotsi, Y.; Yazicioglu, A. G.; Megaridis, C. M.; Yoshimura, M. *Nano Lett.* **2004**, *4*, 2237–2243.

(25) Gogotsi, Y.; Libera, J. A.; Güvenç-Yazicioglu, A.; Megaridis, C. M. *Appl. Phys. Lett.* **2001**, *79*, 1021–1023.

(26) Lech, F. J.; Wierenga, P. A.; Gruppen, H.; Meinders, M. B. J. *Langmuir* **2015**, *31*, 2777–2782.

(27) Ajayan, P. M.; lijima, S. *Nature* **1993**, *361*, 333–334.

(28) Israelachvili, J. N. *Intermolecular and surface forces*, 3rd ed.; Academic press, 2011.

(29) Carey, V. P. *Liquid-vapor phase-change phenomena*, 2nd ed.; Hemisphere, New York, NY (United States), 1992.

(30) Grogan, J. M.; Schneider, N. M.; Ross, F. M.; Bau, H. H. *Nano Lett.* **2014**, *14*, 359–364.

(31) Hu, H.; Weinberger, C. R.; Sun, Y. *Nano Lett.* **2014**, *14*, 7131–7137.

(32) Rafiee, J.; Mi, X.; Gullapalli, H.; Thomas, A. V.; Yavari, F.; Shi, Y.; Ajayan, P. M.; Koratkar, N. A. *Nat. Mater.* **2012**, *11*, 217–222.

(33) Zhao, N.; He, C.; Li, J.; Jiang, Z.; Li, Y. *Mater. Res. Bull.* **2006**, *41*, 2204–2209.

(34) Chaban, V. V.; Prezhdo, V. V.; Prezhdo, O. V. *ACS Nano* **2012**, *6*, 2766–2773.

(35) Peng, T.; Peng, K.; Li, Q. *J. Phys. Chem. C* **2015**, *119*, 14273–14280.

(36) Endo, M.; Kim, Y. A.; Hayashi, T.; Fukai, Y.; Oshida, K.; Terrones, M.; Yanagisawa, T.; Higaki, S.; Dresselhaus, M. S. *Appl. Phys. Lett.* **2002**, *80*, 1267–1269.

(37) Askounis, A.; Yamada, Y.; Ikuta, T.; Takahashi, K.; Takata, Y.; Sefiane, K. *AIP Adv.* **2016**, *6*, 115119.

(38) Yamada, Y.; Askounis, A.; Ikuta, T.; Takahashi, K.; Takata, Y.; Sefiane, K. *J. Appl. Phys.* **2017**, *121*, 15104.

(39) Dujardin, E.; Ebbesen, T. W.; Hiura, H.; Tanigaki, K. *Science* **1994**, *265*, 1850–1852.